Parametric study of a dual-band quasi-Yagi antenna for LTE application

Md. Ashraful Haque[1,2], Mohd Azman Zakariya[1,3], Narinderjit Singh Sawaran Singh[4], Md. Afzalur Rahman[2], Liton Chandra Paul[5]

[1]Department of Electrical and Electronic Engineering, Universiti Teknologi Petronas, Perak, Malaysia
[2]Department of Electrical and Electronic Engineering, Daffodil International University, Dhaka, Bangladesh
[3]Smart Infrastructure Modelling and Monitoring (SIMM) Research Group, Institute of Transportation and Infrastructure, Universiti Teknologi Petronas, Perak, Malaysia
[4]Faculty of Data Science and Information Technology, INTI International University, Persiaran Perdana BBN, Negeri Sembilan, Malaysia
[5]Department of Electrical, Electronic, and Communication Engineering, Pabna University of Science and Technology, Pabna, Bangladesh

Article Info

Article history:

Received Aug 26, 2022
Revised Nov 25, 2022
Accepted Dec 23, 2022

Keywords:

Co-planar stripline
Long-term evolution
Microstrip patch
Quasi-Yagi
Yagi antenna

ABSTRACT

Due to small size and lightweight properties, the development of microstrip (MS) patch antennas for wireless communication has become one of the mobile application devices in demand in recent years. This has helped to reduce reliance on wired cables. In this paper, a study has been performed on MS antenna by developing a quasi-Yagi structure on a fire retardant-4 (FR-4) substrate with a MS to coplanar strip line (CPS) transition feeding technique. The antenna is designed by using computer simulation technology (CST) to achieve the desired resonant frequency and bandwidth. The proposed dual band quasi-Yagi antenna has impedance bandwidths of approximately 0.3 GHz and 0.22 GHz resonating at 1.80 GHz and 2.60 GHz, respectively, which makes it suitable for long-term evolution (LTE) applications. Eight-director elements in four pairs are constructed to achieve directivity with magnitudes of 6 dB and 8.3 dBi at both resonant frequencies, 1.80 GHz and 2.60 GHz, respectively. Different parametric studies have also been performed to characterize the antenna radiation characteristics. The return loss, voltage standing wave ratio (VSWR), front to back (F/B) ratio and far-field radiation are analyzed and discussed.

Corresponding Author:

Narinderjit Singh Sawaran Singh
Faculty of Data Science and Information Technology, INTI International University
Persiaran Perdana BBN, Putra Nilai, Nilai 71800, Negeri Sembilan, Malaysia
Email: narinderjits.sawaran@newinti.edu.my

1. INTRODUCTION

Microstrip (MS) patch antenna is widely utilized in wireless applications because of its compact size, lightweight, and inexpensive construction cost [1]-[5]. This reduces the dependencies on the wired cables hence occupies less space. The number of people using smartphones, computers, smart TVs, and many other internet-connected wireless devices is rising rapidly. The need for creating high-speed wireless networks has increased in response to this enormous number of wireless devices [6]. Today's cellular technology is developing quickly, and we rely on it to withstand our heavy use. Most mobile users and the IoT are adopting the newest technologies in this area because of the necessity for rapid data transfer [7], [8]. MS patch antennas can be designed with different design structures such as rectangular, circular, triangular, square, elliptical, dipole, hexagonal, pentagonal, disk sector, ring sector, rhombic, circular ring, different alphabet shaped, plus shaped, and more to produce different performance levels [9], [10].

The design of a patch antenna can also be derived from a conventional dipole Yagi-Uda antenna, which is comprised of two primary components: supply-driven elements and non-driven parasitic elements, which include reflector and director elements, as depicted in Figure 1. A Yagi-Uda antenna is known for its high gain and narrower bandwidth, which can be controlled by manipulating its simple dipole array structure. Different design techniques for a quasi-Yagi antenna have been presented with different performance levels and radiation characteristics [11]-[15]. The feeding techniques demonstrated for MS antennas can be applied to any quasi-Yagi design [16]-[23]. The proposed layout makes use of a transition feeding method between MS and coplanar strip line (CPS). By adjusting the dimensions of the antenna's quasi-structure, the resonant frequency can be adjusted. The CST software is used to model the quasi-Yagi antenna and to estimate return loss, radiation pattern, gain and directivity of the antenna. The purpose of this research is to propose a quasi-Yagi antenna with high gain and broad bandwidth that could be used in the long-term evolution (LTE) spectrum.

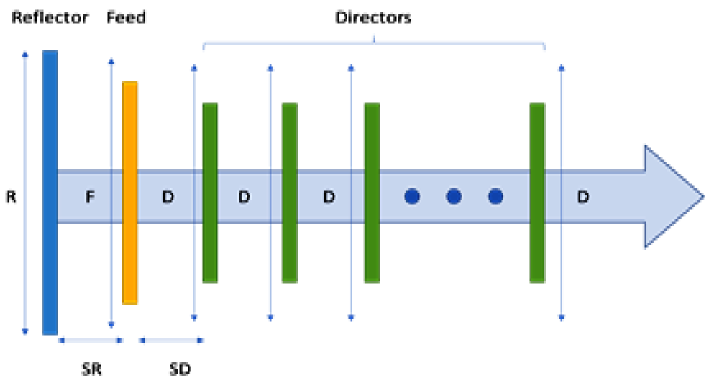

Figure 1. Geometry of a Yagi-Uda antenna

2. PROPOSED QUASI-YAGI ANTENNA CONFIGURATION

A dual band quasi-Yagi antenna has been designed and simulated which is optimized for the LTE band. This antenna would be able to transmit and receive signals at 1.66–2.19 GHz and 2.44–2.66 GHz, respectively. The proposed antenna structure includes a driven element, the eight director elements, and a truncated ground plane made of copper metal, which serves as a reflector element, as shown in Figure 2(a) and Figure 2(b).

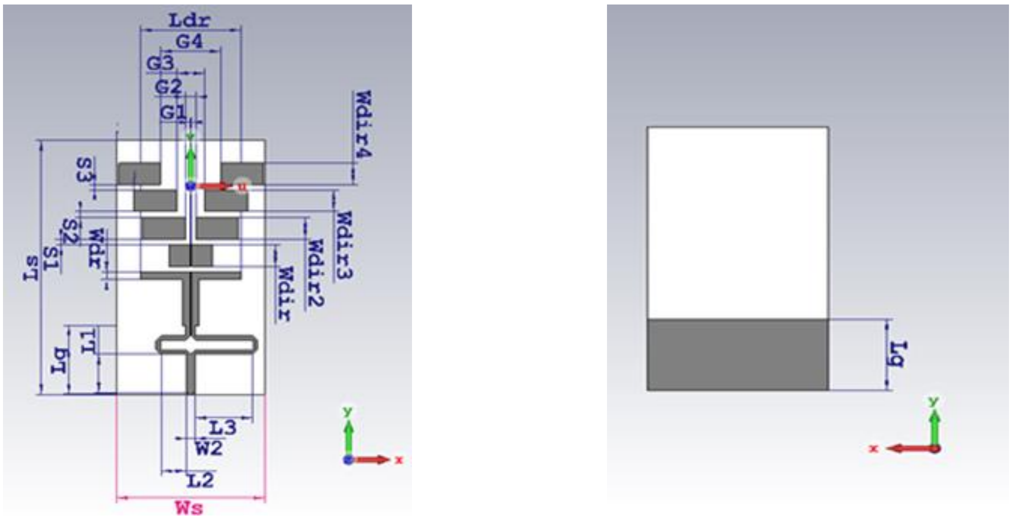

(a) (b)

Figure 2. Geometry of the proposed quasi-Yagi antenna (a) front view and (b) back view

Fire retardant-4 (FR-4) is the antenna substrate material, and its dielectric constant is 4.3 and its thickness is 1.56 mm. In the configuration, the MS dipole is employed to produce a TE0 mode with the electric vector (E) perpendicular to the propagation axis. Transmission line model can be used to design the driven element. The following describe the calculation of λ, L_{dr} and W_{dr}:

$$\varepsilon_{eff} = \frac{\varepsilon_r+1}{2} + \frac{\varepsilon_r-1}{2}\left(\frac{1}{\sqrt{1+\frac{12d}{W_{dr}}}}\right) \tag{1}$$

Where, ε_r=dielectric constant, d=substrate thickness, and W_{dr}=width of the driven element.
The length of the driven element (L_{dr}) is half the wavelength which can be calculated using (2):

$$\lambda = \frac{c}{f\sqrt{\varepsilon_{eff}}} \tag{2}$$

Where λ=wavelength in meter, c=speed of light, and f=frequency.

Conventional feeding techniques using MS lines have an unbalanced characteristic that can affect the radiation of a printed dipole element. Thus, a CPS transition is used to avoid unwanted radiation. Because the CPS line only accepts even mode, a balun phase shifter is used to balance the CPS feeding by generating a 180° phase difference between MS and CPS at both resonant frequencies of 1.80 GHz and 2.60 GHz [24]. This can be achieved by adjusting the length of the delay line on one of the branches such that:

$$\frac{\lambda_g}{4} = L_3 - L_2 \tag{3}$$

$$\lambda_g = \frac{c}{f} \times \frac{1}{\sqrt{1-\left(\frac{c}{2a\times f}\right)^2}} \tag{4}$$

Where, a=width of MS line.

A quarter-wave transformer line with characteristic impedance of Z_0 is utilized to match the 50 Ω port impedance to the 25 Ω T-junction [25]. Using the following equation, the Z_0 with length of λg/4 is 35.35 Ω.

$$Z_0 = \sqrt{Z_{in} Z_L} \tag{5}$$

Where, Z_{in}=input impedance, Z_L=load impedance.

To ensure the antenna is optimized for the required LTE frequency band, it is necessary to do study on the antenna's design parameters including effect of number of director element, effect of tuning ground plane (reflector) length, effect on tuning length of driven element and effect of dielectric thickness. The antenna is 180.13 mm in length and 99.59 mm in width. CST software is used to increase the length of the driven element from its original value of 58.25 mm (based on the formula presented in (1) to (5)) to 71.20 mm. The ground plane with length and width of 43.50 mm and 99.59 mm, respectively, acts as a reflector element to enhance the radiation beam at the plane of the driven element. Four paired i.e. eight director elements are vertically spaced by S1, S2, and S3 respectively and horizontally spaced by G1, G2, G3, and G4 respectively. These spacing are optimized and determined to provide higher gain of the antenna in the LTE operating frequency range. The geometrical parameters for the proposed quasi-Yagi antenna design are listed in Table 1. Figure 3(a) and 3(b) show the front view and back view of the fabricated quasi-Yagi antenna.

Table 1. Geometrical parameters of the quasi-Yagi antenna

Name	Value	Name	Value	Name	Value	Name	Value	Name	Value
W_{dr}	5.50 mm	L_{dir1}	36.07 mm	t	1.56 mm	L_1	29.03 mm	S_3	4.29 mm
L_{dr}	71.20 mm	L_{dir2}	56.99 mm	h	0.02 mm	L_2	21.75 mm	G_1	0.50 mm
W_{dir1}	15.38 mm	L_{dir3}	57.52 mm	W_s	99.59 mm	L_3	43.50 mm	G_2	7.47 mm
W_{dir2}	15.38 mm	L_{dir4}	56.48 mm	L_s	180.13 mm	S_1	3.51 mm	G_3	18.88 mm
W_{dir3}	15.38 mm	W_2	5.90 mm	L_g	48.90 mm	S_2	4.18 mm	G_4	40.34 mm
W_{dir4}	15.38 mm	-	-		-		-	-	-

(a) (b)

Figure 3. Fabricated prototype of the quasi-Yagi antenna (a) front view and (b) back view

3. RESULTS AND DISCUSSION

The amount of power reflected by a transmission line is measured by its return loss (S11). When the magnitude of S11 is lower than -10 dB then the antenna reflects as little energy as possible. The optimized quasi-Yagi antenna has two resonance frequencies of 1.80 GHz and 2.60 GHz, and a graph of the simulated return loss within the range of 1.6 GHz to 3 GHz is shown in Figure 4. First resonant at 1.80 GHz has a return loss of -65.23 dB, and the other at 2.60 GHz has -31.55 dB. Voltage standing wave ratio (VSWR) measures voltage variances along the transmission line. The standard set for an antenna requires a VSWR to be less than 2 for the least variances equivalent to minimum -10 dB level of S11 which is depicted in Figure 5. The gain and directional nature of the quasi-Yagi antenna in both operating bands are depicted in Figure 6. The antenna has a peak gain of 6 dB and a directivity of 8.3 dBi.

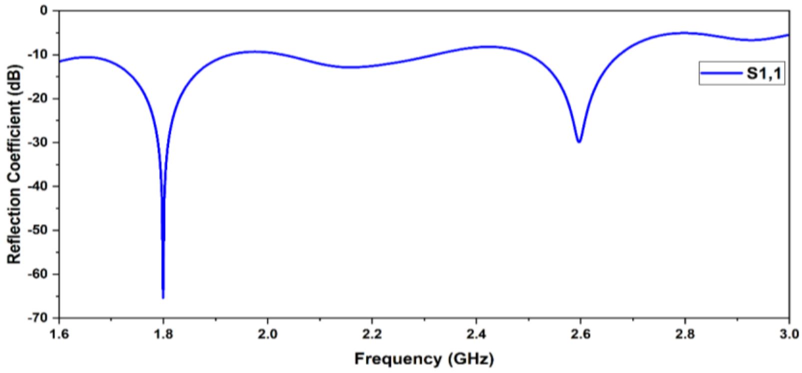

Figure 4. S11 parameter of the quasi-Yagi antenna

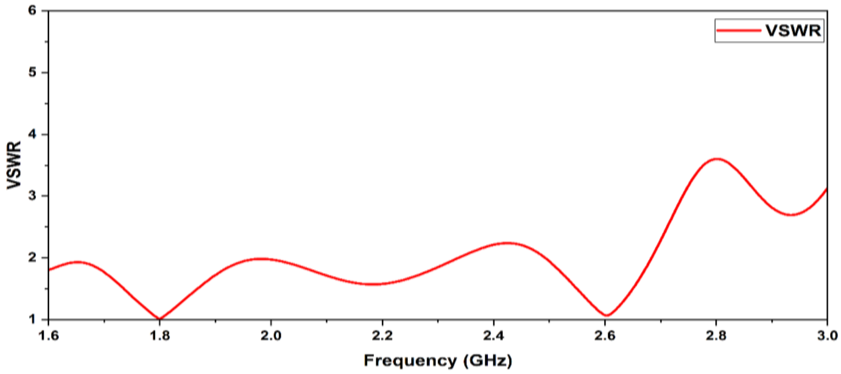

Figure 5. VSWR of the quasi-Yagi antenna

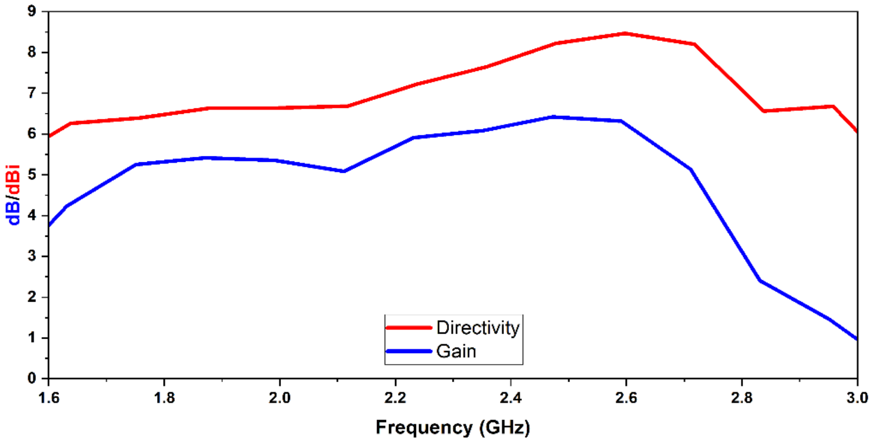

Figure 6. Gain and directivity of the quasi-Yagi antenna

Figure 7(a) and 7(b) depict magnetic and electric fields at an angle of theta equal to 90^0 and an angle of φ equal to 0^0 and 90^0. At the 1.80 resonant frequency, both the E-field and H-prominent field's lobes are centered at 4^0, 83^0, 83^0 for φ=0^0, 90^0 and theta=90^0. The magnitudes of E-fields are -39.9 dBV/m, -31.8 dBV/m, -31.7 dBV/m at φ=0^0, 90^0 and theta=90^0. The -3 dB angular beamwidth, or half power beamwidth is located at 83.6^0, 123.2^0, 74.8^0 and the side lobe level is -13.7 dB, -15.2 dB, -14.1 dB at φ=0^0, 90^0 and theta=90^0. According to the arrangement of the omnidirectional radiation patterns, the Yagi antenna emits radiation in all directions that are perpendicular to the x-axis. Analysis shows that this omnidirectional Yagi antenna is a good option for LTE networks.

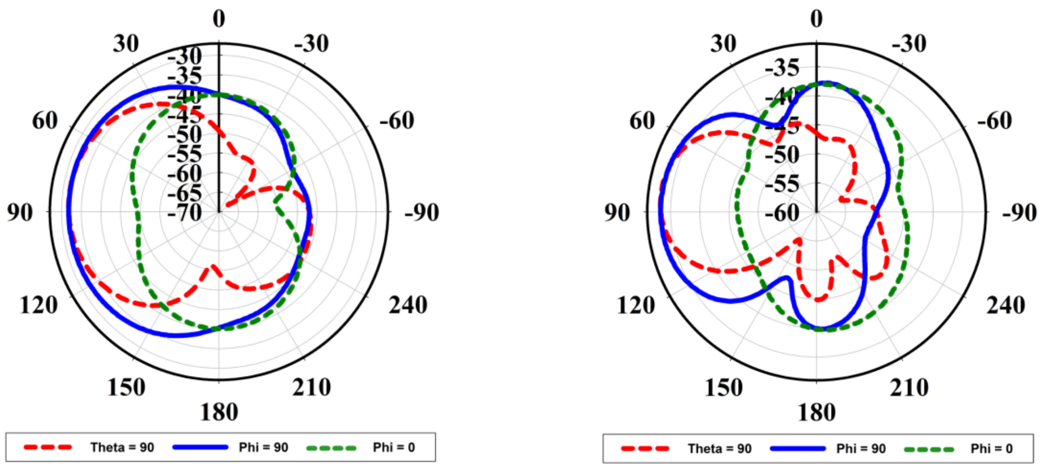

(a) (b)

Figure 7. Radiation patterns of the quasi-Yagi antenna at (a) 1.80 GHz and (b) 2.60 GHz

4. PARAMETRIC ANALYSIS

The effectiveness of a MS type Yagi-Uda antenna depends on several factors, including the substrate's thickness, the lengths of the feed and parasitic components, and the spacing between them. To get the best possible results from an antenna, it is important to determine its geometrical factors through an exhaustive parametric analysis. In this research work, we have conducted an exhaustive parametric study to investigate how the geometrical factors impact the antenna's outgoing signal.

4.1. Effect of changing the number of director elements

There are two scenarios that are being investigated in this study. The first scenario evaluates the radiation characteristic of the antenna for a different number of director elements (in pairs) along symmetrical lines at G1, G2, G3, and G4. The result of the variation can be depicted in Figure 8. As the number of director elements increases, the first resonant point is shifted significantly. The reflection coefficients for first resonant frequency are -19 dB, -24 dB, -54 dB, -45 dB, and -67 dB for 0, 1, 2, 3, and 4 number directors, respectively. At higher frequency, the second resonant frequency of 2.60 GHz does not show any significant frequency shift with the number of elements, but the magnitude varies such as -20 dB, -40 dB, -26 dB, -30 dB, and -35 dB for 0, 1, 2, 3, and 4 number directors. The magnitude variation for both frequencies are influenced by the antenna impedance which can be further studied in a smith chart plot. In this case the eight director element antenna has an impedance of 50 Ω at the resonant frequencies.

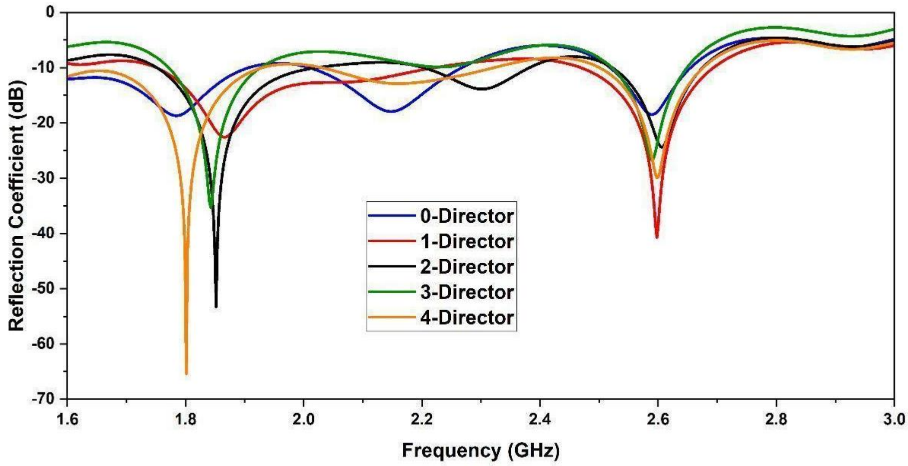

Figure 8. Effect of changing the number of directors on S11

4.2. Effect of tuning ground plane (reflector) length, L_g

With this adjustment, the ground plane length goes up from 48.9-56.9 mm, an increment of 2 mm in each step. Figure 9 demonstrates the return loss (S11) where the magnitude of S11 reduces and shifts to the left for the first resonant frequency while increasing the length of the ground plane (L_g). For the higher resonant frequency, the return loss also slightly varies, and the resonant frequency significantly shifts to the left of 2.6 GHz. Front to back (F/B) ratio and directivity are also investigated for both frequencies. Table 2 summarizes the results obtained from the study. It shows that, at 1.80 GHz, initially the F/B ratio increases from 13.47-13.61 dB then decreases to 12.76 dB while increasing the length of the L_g from 48.90 mm to 56.90 mm. In the same fashion, at 1.80 GHz, the directivity also increases from 6.63 dBi to 6.74 dBi then decreases to 6.5 dBi. For resonant frequency of 2.60 GHz, initially the F/B increases and later decreases whereas the directivity decreases with increasing the length of L_g. The decrease in F/B is due to increasing back lobe of the radiation since the partial ground plane act as the reflector element.

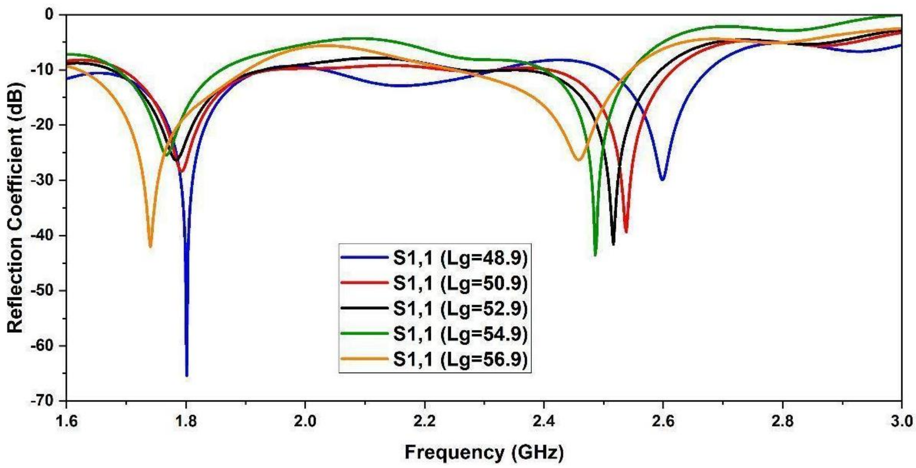

Figure 9. Effect of tuning ground plane length (L_g) on S11

Table 2. Front-to-back (F/B) ratio and directivity with varying the length of L_g

Resonant frequency	1.80 GHz		2.60 GHz	
L_g (mm)	F/B (dB)	Directivity (dBi)	F/B (dB)	Directivity (dBi)
48.90	13.47	6.63	14.96	8.30
50.90	13.51	6.69	15.39	8.01
52.90	13.61	6.74	15.25	7.96
54.90	13.40	6.71	14.46	7.80
56.90	12.76	6.50	13.09	7.31

4.3. Effect of tuning length of driven element (L_{dr})

The length of the driving element is varied from 63.20-71.20 mm in this study. Figure 10 demonstrates that the first resonant frequency significantly changes with the change of driven element length (L_{dr}) whereas the second resonant frequency remains almost fixed at 2.60 GHz. The quasi-Yagi antenna resonates at 1.80 GHz and 2.60 GHz with most suitable bandwidths and reflection coefficients for desired LTE spectrum. The reflection coefficients are -67 dB and -35 dB at 1.80 GHz and 2.60 GHz, respectively, for 71.20 mm length of driven element.

4.4. Effect of substrate thickness (t)

Return loss for various substrate thicknesses (t) is depicted in Figure 11. The thickness of the FR-4 substrate is varied from 1.56-1.76 mm. As the substrate's thickness grows, the quasi-Yagi antenna's resonant frequencies and bandwidths shift significantly. For the thickness of 1.56 mmm, the designed quasi-Yagi antenna resonates at the intended frequencies of 1.80 GHz and 2.60 GHz with good reflection coefficients.

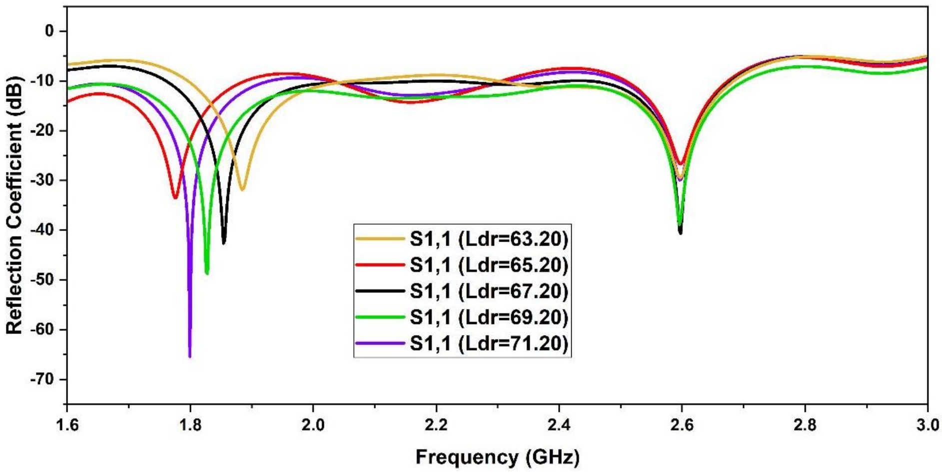

Figure 10. Effect of tuning driven element length (L_{dr}) on S11

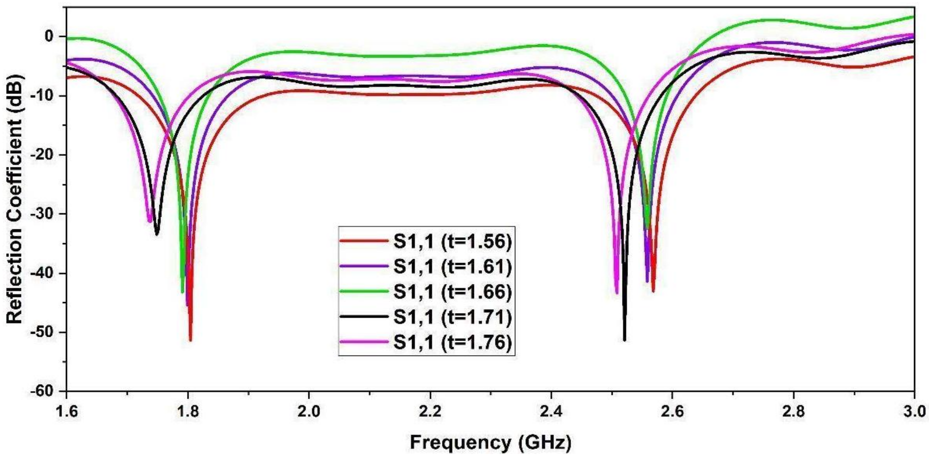

Figure 11. Effect of changing substrate thickness (t) on S11

5. CONCLUSION

In this work, we have presented a dual-band quasi-Yagi antenna with eight directors. The proposed quasi-Yagi antenna features a dual resonant frequency of 1.80 GHz and 2.60 GHz respectively. In order to characterize the designed antenna, different parametric studies including effect of number of directors, length of reflector (L_g), driven element (L_{dr}) and thickness of substrate (t) have been conducted. CST software is used to design and examine the aforementioned studies of different parameters. The prototype of the designed quasi-Yagi antenna has been developed in the laboratory. The quasi-Yagi antenna shows good reflection coefficient, gain, directivity, (F/B) ratio and VSWR for the both operating bands of 1.80 GHz and 2.60 GHz. The proposed design may be suitable for the LTE band of mobile communications.

ACKNOWLEDGEMENTS

The author thanks all colleagues for their support, supervision, advice, and project information. The author would also like to thank Communication Lab Technologists of University Technology Petronas (UTP) group and Agriculture IOT (AIOT) Research Group, Institute of Transportation, and Infrastructure, Universiti Teknologi PETRONAS, and the Faculty of Data Science and Information Technology at INTI International University, Malaysia, for providing state-of-the-art research facilities. The author thanks UTP Electrical and Electronics Engineering for allowing him to work on this project, which improved his technical and problem-solving skills.

REFERENCES

[1] S. Parasuraman, S. Yogeeswaran, and G. P. Ramesh, “Design of Microstrip Patch Antenna with improved characteristics and its performance at 5.1GHz for Wireless Applications,” *IOP Conference Series: Materials Science and Engineering*, vol. 925, no. 1, p. 012005, Sep. 2020, doi: 10.1088/1757-899x/925/1/012005.

[2] L. C. Paul, H. K. Saha, T. Rani, M. Z. Mahmud, T. K. Roy, and W.-S. Lee, “An Omni-Directional Wideband Patch Antenna with Parasitic Elements for GHz Band Applications,” *International Journal of Antennas and Propagation*, vol. 2022, pp. 1–11, Oct. 2022, doi: 10.1155/2022/9645280.

[3] A. Arif, M. Zubair, M. Ali, M. U. Khan, and M. Q. Mehmood, “A Compact, Low-Profile Fractal Antenna for Wearable On-Body WBAN Applications,” *IEEE Antennas and Wireless Propagation Letters*, vol. 18, no. 5, pp. 981–985, May 2019, doi: 10.1109/lawp.2019.2906829.

[4] L. C. Paul, H. K. Saha, T. Rani, R. Azim, M. T. Islam, and M. Samsuzzaman, “A dual-band semi-circular patch antenna for WiMAX and WiFi-5/6 applications,” *International Journal of Communication Systems*, vol. 36, no. 1, Oct. 2022, doi: 10.1002/dac.5357.

[5] H. Liu, A. Qing, Z. Xu, Z. Yu, and S. Zhang, “Design of Physically Connected Wideband SIW Cavity-Backed Patch Antenna for Wide-Angle Scanning Phased Arrays,” *IEEE Antennas and Wireless Propagation Letters*, vol. 20, no. 3, pp. 406–410, Mar. 2021, doi: 10.1109/lawp.2021.3053413.

[6] H. Zhang, N. Liu, X. Chu, K. Long, A.-H. Aghvami, and V. C. M. Leung, “Network Slicing Based 5G and Future Mobile Networks: Mobility, Resource Management, and Challenges,” *IEEE Communications Magazine*, vol. 55, no. 8, pp. 138–145, Aug. 2017, doi: 10.1109/mcom.2017.1600940.

[7] M. Attaran, “The impact of 5G on the evolution of intelligent automation and industry digitization,” *Journal of Ambient Intelligence and Humanized Computing*, Feb. 2021, doi: 10.1007/s12652-020-02521-x.

[8] S. Kannadhasan and R. Nagarajan, “Performance Analysis of Circular Shape Microstrip Antenna for Wireless Communication System,” *IOP Conference Series: Materials Science and Engineering*, vol. 1085, no. 1, p. 012013, Feb. 2021, doi: 10.1088/1757-899x/1085/1/012013.

[9] L. C. Paul, M. T. R. Jim, T. Rani, S. S. A. Ankan, S. C. Das, and H. K. Saha, “A Π-shaped Slotted Patch Antenna with a Partial Ground Structure for Lower 5G/WiFi/WiMAX Applications,” *Heliyon*, vol. 8, no. 10, p. e10934, Oct. 2022, doi: 10.1016/j.heliyon.2022.e10934.

[10] E. Gupta, S. K. Kundu, S. Rawat, and P. K. Singhal, “Circularly Polarized Planar and Curve structured antenna using symmetrical crossed elliptical slots,” *Wireless Personal Communications*, Sep. 2022, doi: 10.1007/s11277-022-09954-x.

[11] Z. Wang, Y. Ning, and Y. Dong, “Compact Shared Aperture Quasi-Yagi Antenna With Pattern Diversity for 5G-NR Applications,” *IEEE Transactions on Antennas and Propagation*, vol. 69, no. 7, pp. 4178–4183, Jul. 2021, doi: 10.1109/tap.2020.3044633.

[12] F. Wei, X.-B. Zhao, and X. W. Shi, “A Balanced Filtering Quasi-Yagi Antenna with Low Cross-Polarization Levels and High Common-Mode Suppression,” *IEEE Access*, vol. 7, pp. 100113–100119, 2019, doi: 10.1109/access.2019.2931141.

[13] S. Fu, A. Xiong, W. Chen, and S. Fang, “A compact planar Moxon-Yagi composite antenna with end-fire radiation for dual-band applications,” *Microwave and Optical Technology Letters*, vol. 62, no. 6, pp. 2328–2334, Jun. 2020, doi: 10.1002/mop.32331.

[14] S.-A. Malakooti, S. M. H. Mousavi, and C. Fumeaux, “Tunable Bandpass-to-Bandstop Quasi-Yagi–Uda Antenna With Sum and Difference Radiation Patterns,” *IEEE Transactions on Antennas and Propagation*, vol. 67, no. 4, pp. 2260–2271, Apr. 2019, doi: 10.1109/tap.2019.2891451.

[15] A. D. Chaudhari and K. P. Ray, “Printed broadband Quasi-Yagi antenna with monopole elements,” *IET Microwaves, Antennas and Propagation*, vol. 14, no. 6, pp. 468–473, Mar. 2020, doi: 10.1049/iet-map.2019.0628.

[16] N. O. Parchin, M. Alibakhshikenari, H. J. Basherlou, R. A. A-Alhameed, J. Rodriguez, and E. Limiti, “MM-Wave Phased Array Quasi-Yagi Antenna for the Upcoming 5G Cellular Communications,” *Applied Sciences*, vol. 9, no. 5, p. 978, Mar. 2019, doi: 10.3390/app9050978.

[17] L. C. Paul, M. M. G. Nabi, M. M. U. Rashid, R. Sen, M. Z. Mahmud, and M. M. Rahman, “Wideband Microstrip Yagi-Uda Array Antenna with High Gain and F/B Ratio for 5 GHz Wi-Fi Band Applications,” in *2018 International Conference on Innovation in Engineering and Technology (ICIET)*, Dec. 2018, doi: 10.1109/ciet.2018.8660877.

[18] S. P-Khanjari, F. B. Zarrabi, and S. Jarchi, "Compact and wide-band Quasi Yagi-Uda antenna based on periodic grating ground and coupling method in terahertz regime," *Optik*, vol. 203, p. 163990, Feb. 2020, doi: 10.1016/j.ijleo.2019.163990.
[19] S. S. Jehangir and M. S. Sharawi, "A Compact Single-Layer Four-Port Orthogonally Polarized Yagi-Like MIMO Antenna System," *IEEE Transactions on Antennas and Propagation*, vol. 68, no. 8, pp. 6372–6377, Aug. 2020, doi: 10.1109/tap.2020.2969810.
[20] S. Liu, R. Raad, P. I. Theoharis, and F. E. Tubbal, "A Printed Yagi Antenna for CubeSat with Multi-Frequency Tilt Operation," *Electronics*, vol. 9, no. 6, p. 986, Jun. 2020, doi: 10.3390/electronics9060986.
[21] M. Gupta and H. Kumar, "Compact and Broadband Uniplanar Quasi-Yagi Microstrip Antenna," in *2021 IEEE Indian Conference on Antennas and Propagation (InCAP)*, Dec. 2021, doi: 10.1109/incap52216.2021.9726395.
[22] H. Das, M. Sharma, and Q. Xu, "Microstrip Antenna: An Overview and Its Performance Parameter," in *Smart Antennas*, Springer International Publishing, 2022, pp. 3–14, doi: 10.1007/978-3-030-76636-8_1.
[23] R. K. Singh, A. Michel, P. Nepa, and A. Salvatore, "Wearable Dual-Band Quasi-Yagi Antenna for UHF-RFID and 2.4 GHz Applications," *IEEE Journal of Radio Frequency Identification*, vol. 4, no. 4, pp. 420–427, Dec. 2020, doi: 10.1109/jrfid.2020.3000298.
[24] M. Elahi, Irfanullah, R. Khan, A. A. Al-Hadi, S. Usman, and P. J. Soh, "A dual-band planar quasi yagi-uda antenna with optimized gain for lte applications," *Progress In Electromagnetics Research C*, vol. 92, pp. 239–250, 2019, doi: 10.2528/pierc19022401.
[25] M. Varan, A. T. Ergüzel, H. H. Genç, B. Ulusoy, I. Öylek, and M. Ay, "Design and implementation of an open source transmission line impedance matching educational framework," *Computer Applications in Engineering Education*, vol. 28, no. 3, pp. 724–736, Apr. 2020, doi: 10.1002/cae.22242.

BIOGRAPHIES OF AUTHORS

Md. Ashraful Haque is doing Ph.D. at the Department of Electrical and Electronic Engineering, Universiti Teknologi PETRONAS, Malaysia, He got his B.Sc. in Electronics and Electronic Engineering (EEE) from Bangladesh's Rajshahi University of Engineering and Technology (RUET) and his M.Sc. in the same field from Bangladesh's Islamic University of Technology (IUT). He is currently on leave from Daffodil International University (DIU) in Bangladesh. His research interest includes microstrip patch antenna, sub 6 5G application, regression model machine learning on antenna design. He can be contacted at email: limon.ashraf@gmail.com.

Mohd Azman Zakariya born in Pahang, Malaysia in 1972 is IEEE member since 2015. He joined Universiti Teknologi PETRONAS in 1999. He is holding a position as Senior Lecturer in the Electrical and Electronic Engineering Department. He obtained the B.Eng. degree in Electrical and Electronic Engineering in 1999 from Universiti Teknologi Malaysia, Malaysia, Master of Science Degree in Communication and Signal Processing in 2001 from University of Newcastle Upon Tyne, and PhD in RF and Microwave in 2015 from Universiti Sains Malaysia. Currently he is assigned as Head of Research Group of Algriculture IOT (AIOT), under Institute of Tranportation and Infrasture (ITI). His research interest is in RF and microwave circuit design, antenna and wireless system and IoT systems. He can be contacted at email: mazman_zakariya@utp.edu.my.

Narinderjit Singh Sawaran Singh is a Senior Lecturer in INTI International University, Malaysia. He graduated from the Universiti Teknologi PETRONAS (UTP) in 2016 with Ph.D in Electrical and Electronic Engineering specialized in Probabilistic Methods for Fault Tolerant Computing. Currently, he is appointed as the research cluster head for Computational Mathematics, Technology and Optimization which focuses on the areas like pattern recognition and symbolic computations, game theory, mathematical artificial intelligence, parallel computing, expert systems and artificial intelligence, quality software, information technology, exploratory data analysis, optimization algorithms, stochastic methods, data modelling and computational intelligence–swarm intelligence. He is one of the appointed Editorial Board Members for Journal of Data Science (JoDS)-an international journal indexed by Google Scholar and MyJurnal. He is a very dedicated and committed academician with 21 years of experience in teaching and more than 10 years of research experience. He is a very resourceful researcher with wideranging research interests-computational, modeling and simulation, mathematical and statistical modeling, fault-tolerant computing (reliability-VLSI circuit design), and healthcare data analysis are on the top of the list. He can be contacted at email: narinderjits.sawaran@newinti.edu.my.

Md. Afzalur Rahman is working as an Assistant Engineer in a consultancy firm named Fire and Electrical Solutions, Dhaka, Bangladesh. He is from Cumilla, Bangladesh. He has completed his B.Sc. in Engineering Degree in Electrical and Electronics Engineering (EEE) from Daffodil International University in 2022. Before that, he completed his Higher Secondary School Certificate from Bangladesh Navy College, Dhaka, Bangladesh, and his Secondary School Certificate from Cumilla Modern High School, Cumilla, Bangladesh. He can be contacted at email: afzalur33-4556@diu.edu.bd.

Liton Chandra Paul (Senior Member, IEEE) is working as a Faculty Member in the department of Electrical, Electronic and Communication Engineering, Pabna University of Science and Technology. He successfully completed B.Sc. in Electronics and Telecommunication Engineering (ETE) and M.Sc. in Electrical and Electronic Engineering from Rajshahi University of Engineering and Technology in 2012 and 2015 respectively. He is the 1st class 1st boy of 3rd batch of the department and awarded as University Gold Medalist for his outstanding academic performance in B.Sc. in ETE. He has published several peer reviewed Journals and Conference articles. He is very enthusiastic to contribute to various voluntary social welfare organizations from his student life. He also serves as a reviewer of several IEEE international conferences and reputed journals. He is connected with different national and international professional body like Institute of Engineers Bangladesh (IEB), Institute of Electrical and Electronics Engineers (IEEE) including IEEE-APS, IEEE-MTTS, IEEE-SPS, IEEE-WIE etc. His research interests are antenna and wave propagation, AI, biomedical engineering and wireless communication. He can be contacted at email: litonpaulete@gmail.com.